SUPPORTING INFORMATION

TABLE OF CONTENTS

1. Synthesis and structural design of VEGF mimics

1.1 Discontinuous mimics 1-8

The binding site of bevacizumab on VEGF is located at the top of the β5-turn-β6 loop of VEGF (85-PHQGQHIG-92)(1). For proper reconstruction of this binding it is important to realize that the binding site is discontinuous in nature, indicating that it includes both the β5-turn-β6 loop as well as the β2-α2-β3-loop. The latter sequence is not in direct contact with the antibody, but it provides structural support to the antibody-binding β5-turn-β6 loop (for schematic illustration, see **Fig. 1B**). Therefore, we constructed the 79-mer peptide covering the native VEGF-sequence from Cys-26 (C_I of cysteine-knot fold) until Cys-104 (C_{VI} of cysteine-knot fold). This peptide (red-**1**) covers approximately 25% of the full-length sequence of native $hVEGF_{165}$ (**Fig. 1C**). To make sure that peptide **1** cannot dimerize during oxidative folding (as native VEGF does), we substituted both the residues Cys-51 and Cys-60 for alanines (**Fig. 1C**). These residues form two native disulfide bonds (one per subunit) that covalently link the individual subunits of the native VEGF homodimer.

1.2 Linear and conformational mimics 9-33

In order to verify whether the bevacizumab binding site on VEGF can also be mimicked efficiently by either cyclic or linear peptide including the 85-PHQGQHIG-92 sequence, we also designed a set of five linear peptides (**9-13**) and twenty xylene-bridged (**14-33**), with different lengths between residues 69 and 103. (**Fig. 1D**). In each of the twenty xylene-bridged peptides an adjacent pair of native amino acids has been replaced by two cysteines (I_{76} and F_{96} for peptides **14-18**, M_{78} and M_{94} for peptides **19-23**, I_{80} and G_{92} for peptides **24-28**, and M_{81} and I_{91} for peptides **29-33**), and the peptides were then cyclized via (intramolecular) reaction with α,α-*meta*-dibromoxylene at both cysteines (2). This approach followed from earlier work from us involving the mimicry of the β3-hairpin loop on Follicle Stimulating Hormone (FSH), which transformed peptides derived from this loop into very potent immunogens that elicited strongly neutralizing and cross-reactive antibodies to another cysteine knot protein, FSH (3).

1.3 Synthesis of VEGF mimics

*1.3.1 Fmoc-synthesis of peptides **1-13***

Peptides were synthesized on solid-phase using a 4-(2',4'-dimethoxyphenyl-Fmoc-aminomethyl)-phenoxy (RinkAmide or Tentagel Amide) resin (BACHEM, Germany) on a Symphony/Prelude (Protein Technologies Inc., USA), Voyager (CEM GmbH, Germany), or SyroII (MultiSyntech, Germany) synthesizer. All Fmoc-amino acids were purchased from Biosolve (Netherlands) or Bachem GmbH (Germany) with side-chain functionalities protected as N-*t*-Boc (KW), O-*t*-Bu (DESTY), N-Trt (HNQ), S-Trt (C), or N-Pbf (R) groups. A coupling protocol using a 5-fold excess of HBTU/HOBt/amino acid/DIPEA (1:1:1:2) in NMP with a 20 minute activation time using double couplings was employed for every amino acid coupling step. Acetylation (Ac) of the peptide was performed by reacting the resin with NMP/Ac_2O/DIEA (10:1:0.1, v/v/v) for 30 min at room temperature. The acetylated peptide was cleaved from the resin by reaction with TFA (40 mL/mmol resin) containing 13.3% (w) phenol, 5% (v) thioanisole, 2.5% (v) 1,2-ethanedithiol, and 5% (v) milliQ-H_2O for 2 hours at room temperature, unless indicated otherwise. Precipitation with ice-cold Et_2O + lyophilization of the precipitated material afforded the crude peptide.

For peptides **1-4, 6** and **7** a low-loaded resin (0.2 mmol/g) was used and the synthesis was performed on a Symphony synthesizer (Protein Technologies Inc., USA). The acylated peptide was cleaved from the resin by reaction with the following cleavage mixture (up to 40 mL/mmol resin): TFA containing 5% (v) TES, 2.5% (v) 1,2-ethanedithiol, and 2.5% (v) milliQ-H_2O. Cleavage reactions took 2-4 hours at room temperature, where after the cleaved peptide was precipitated from the reaction mixture by addition of an excess of ether/pentane 1:1 (v/v). After filtration of the precipitated peptides and freeze-drying from a mixture of ACN/H_2O, the peptides were purified by preparative RP-HPLC.

*1.3.2 Oxidative folding of peptides **1-4**, **6** and **7***

Fully reduced peptides **1-4, 6** and **7** were dissolved in 0.1 M Tris-buffer (pH 8.0), with or without 1M guanidine.HCl, containing 1.0 mM cysteine (SS-form) and 8.0 mM cysteine (SH-form) in a final concentration of 0.1 mg/mL and stirred at room temperature. Immediately, a sharp peak appeared at a lower retention time (more polar) in addition to some broad peaks that correspond to incomplete or incorrectly folded peptide. When HPLC-analysis showed no further change in peak intensities (usually after ~4 hours), the mixture was loaded onto a preparative RP/C_{18} column and purified by preparative RP-HPLC.

*1.3.3 Iodoacetamidation of (reduced) peptide **1** to give peptide **5***

Peptide **1** was iodoacetamidated by addition of a slight excess (~10 equiv.) of iodoacetamide (MW 184.96) to a 1-5 mM solution of the peptide in ACN/milliQ 1:1 (v/v). Then, ammonium bicarbonate (200 mM) was added to this solution until pH= 8. After one hour reaction at room temperature the conversion was complete and the peptide was diluted with milliQ and loaded onto a preparative RP-HPLC column and purified. This peptide (number **5**) served as a negative control of peptide **1**, as it is no longer able to fold and/or form the native SS-bonds because the cysteines have all been capped with $AcNH_2$ groups.

Table S1. Sequence information for peptides **1-8**

Nr	Peptide sequence[a]	Residues	Species	SS-bonds	Acronym
1	*CHPIETLVDIFQEYPDEIEYIFKPSAVPLMRCGGACNDEGLECVPTEESNITMQIMRIKPHQGQHIGEMSFLQHNKCEC#	26-104	human	3	Ox-hVEGF$_{26-104}$
2	***A**HPIETLVDIFQEYPDEIEYIFKPSAVPLMRCGGACNDEGLE**A**VPTEESNITMQIMRIKPHQGQHIGEMSFLQHNKCEC#	26-104	human	2	SS-del1
3	*CHPIETLVDIFQEYPDEIEYIFKPSAVPLMR**A**GGACNDEGLECVPTEESNITMQIMRIKPHQGQHIGEMSFLQHNK**A**EC#	26-104	human	2	SS-del2
4	*CHPIETLVDIFQEYPDEIEYIFKPSAVPLMRCGGA**A**NDEGLECVPTEESNITMQIMRIKPHQGQHIGEMSFLQHNKCE**A**#	26-104	human	2	SS-del3
5	***X**HPIETLVDIFQEYPDEIEYIFKPSAVPLMR**X**GGA**X**NDEGLE**X**VPTEESNITMQIMRIKPHQGQHIGEMSFLQHNK**X**E**X**#[b]	26-104	human	0	IAM$_6$-hVEGF$_{26-104}$
6	*CRPIETLVDIFQEYPDEIEYIFKPSAVPLMRCAGACNDEALECVPTSESNVTMQIMRIKPHQSQHIGEMSFLQHSRCEC#	26-104	rat	3	Ox-rVEGF$_{26-104}$
7	*CRPIETLVDIFQEYPDEIEYIFKPSAVPLMRCAGACNDEALECVPTSESNITMQIMRIKPHQSQHIGEMSFLQHSRCEC#	26-104	mouse	3	Ox-mVEGF$_{26-104}$
8	*XRPIETLVDIFQEYPDEIEYIFKPSAVPLMRXAGAXNDEALEXVPTSESNITMQIMRIKPHQSQHIGEMSFLQHSRXEX#	26-104	mouse	0	IAM$_6$-mVEGF$_{26-104}$

a) '*' denotes N-terminal acetylation; '#' denotes C-terminal amide; b) X = Cys[CH_2(C=O)NH_2]

Table S2. UPLC/ESI-MS analysis data for peptides **1-8**

Nr	Specifics	Species	R_f (%ACN)	MW_{calc} (Da)	MW_{exp} (Da)
1	(reduced, free SH)	human	44,8	9065,5	9066,4
1	(oxidized, SS)	human	39,8	9059,5	9059,1
2	(reduced, free SH)	human	44,3	9001,5	9002,5
2	(oxidized, SS)	human	43,5	8997,4	8998,3
3	(reduced, free SH)	human	44,8	9001,5	9002,1
3	(oxidized, SS)	human	42,8	8997,4	8996,4
4	(reduced, free SH)	human	44,8	9001,5	9002,0
4	(oxidized, SS)	human	43,3	8997,4	8998,6
5		human	43,0	9407,9	9410,3
6	(reduced, free SH)	rat	45,8	9087,7	9088,0
6	(oxidized, SS)	rat	39,5	9081,6	9082,6

7	(reduced, free SH)	mouse	45,5	9101,7	9102,6
7	(oxidized, SS)	mouse	39,5	9095,6	9096,3
8	(denatured, 6x IAM)	mouse	43,3	9443,9	9444,8

*1.3.4 Xylene-bridged peptides **14-33***

The dicysteine peptides **14-33** were all cyclized by reaction with a 1.25 molar excess of *meta*-dibromoxylene following the procedure as described by Timmerman *et al* (3).

Table S3. Sequence and analysis data for peptides **9-33**

Nr	Peptide Sequence[a]	Residues	Xylene bridge[b]	R_f (%ACN)	MW_{calc} (Da)	MW_{exp} (Da)
9	*ESNITMQIMRIKPHQGQHIGEMSFLQH#	73-99	n.a.	30,0	3232,9	3231,1
10	*EESNITMQIMRIKPHQGQHIGEMSFLQHN#	72-100	n.a.	29,7	3474,1	3474,6
11	*TEESNITMQIMRIKPHQGQHIGEMSFLQHNK#	71-101	n.a.	29,1	3705,4	3703,9
12	*PTEESNITMQIMRIKPHQGQHIGEMSFLQHNKA#	70-102	n.a.	29,5	3873,6	3872,2
13	*VPTEESNITMQIMRIKPHQGQHIGEMSFLQHNKAE#	69-103	n.a.	30,1	4101,8	4100,5
14	*ESN**C**TMQIMRIKPHQGQHIGEMS**C**LQH#	73-99	76-96	27,7	3281,0	3279,6
15	*EESN**C**TMQIMRIKPHQGQHIGEMS**C**LQHN#	72-100	76-96	27,4	3524,2	3524,1
16	*TEESN**C**TMQIMRIKPHQGQHIGEMS**C**LQHNK#	71-101	76-96	26,8	3753,5	3753,3
17	*PTEESN**C**TMQIMRIKPHQGQHIGEMS**C**LQHNKA#	70-102	76-96	27,2	3921,7	3920,8
18	*VPTEESN**C**TMQIMRIKPHQGQHIGEMS**C**LQHNKAE#	69-103	76-96	27,7	4149,9	4149,3
19	*ESNIT**C**QIMRIKPHQGQHIGE**C**SFLQH#	73-99	78-94	28,9	3278,9	3278,6
20	*EESNIT**C**QIMRIKPHQGQHIGE**C**SFLQHN#	72-100	78-94	28,4	3522,1	3521,7
21	*TEESNIT**C**QIMRIKPHQGQHIGE**C**SFLQHNK#	71-101	78-94	27,7	3751,4	3751,1
22	*PTEESNIT**C**QIMRIKPHQGQHIGE**C**SFLQHNKA#	70-102	78-94	28,2	3919,6	3919,3
23	*VPTEESNIT**C**QIMRIKPHQGQHIGE**C**SFLQHNKAE#	69-103	78-94	28,6	4147,9	4147,6
24	*ESNITMQ**C**MRIKPHQGQHI**C**EMSFLQH#	73-99	80-92	29,4	3371,1	3370,9
25	*EESNITMQ**C**MRIKPHQGQHI**C**EMSFLQHN#	72-100	80-92	29,0	3614,3	3613,4
26	*TEESNITMQ**C**MRIKPHQGQHI**C**EMSFLQHNK#	71-101	80-92	28,3	3843,6	3843,0
27	*PTEESNITMQ**C**MRIKPHQGQHI**C**EMSFLQHNKA#	70-102	80-92	28,6	4011,8	4010,7
28	*VPTEESNITMQ**C**MRIKPHQGQHI**C**EMSFLQHNKAE#	69-103	80-92	29,1	4240,0	4239,9
29	*ESNITMQI**C**RIKPHQGQH**C**GEMSFLQH#	73-99	81-91	28,4	3297,0	3296,5
30	*EESNITMQI**C**RIKPHQGQH**C**GEMSFLQHN#	72-100	81-91	28,1	3540,2	3540,1
31	*TEESNITMQI**C**RIKPHQGQH**C**GEMSFLQHNK#	71-101	81-91	27,4	3769,5	3768,6
32	*PTEESNITMQI**C**RIKPHQGQH**C**GEMSFLQHNKA#	70-102	81-91	27,8	3937,6	3937,4
33	*VPTEESNITMQI**C**RIKPHQGQH**C**GEMSFLQHNKAE#	69-103	81-91	28,3	4165,9	4165,1

a) '*' denotes N-terminal acetylation; '#' denotes C-terminal amide; b) the xylene-bridge used to connect the cysteines is *meta*-dibromoxylene.

1.3.5 Purification of peptides using preparative RP-HPLC

This was performed according to the procedure as described by Timmerman *et al* (3).

1.3.6 RP-HPLC analysis

Analysis of the purified peptide was performed by reversed-phase high performance liquid chromatography (RP-HPLC) on an Acquity UPLC (Waters, USA) using a RP-18 preparative "BEH" column (2.1x50 inner diameter, 1.7 mm particle size, Waters, USA) with a linear AB gradient (5-55% B, 25% B/min), where solvent A was 0.05% TFA in water and solvent B was 0.05% TFA in ACN. The primary ion molecular weight of the peptides was determined by electron-spray ionization mass spectrometry (ESI-MS).

1.3.7 ESI-MS-analysis

Electrospray ionization mass spectrometry (ESI-MS) of HPLC samples was performed on an API-150 single quadrupole mass spectrometer (Applied Biosystems). Peptide masses were calculated from the experimental mass to charge (*m/z*) ratios from all the observed protonation states of a peptide using Analysis software.

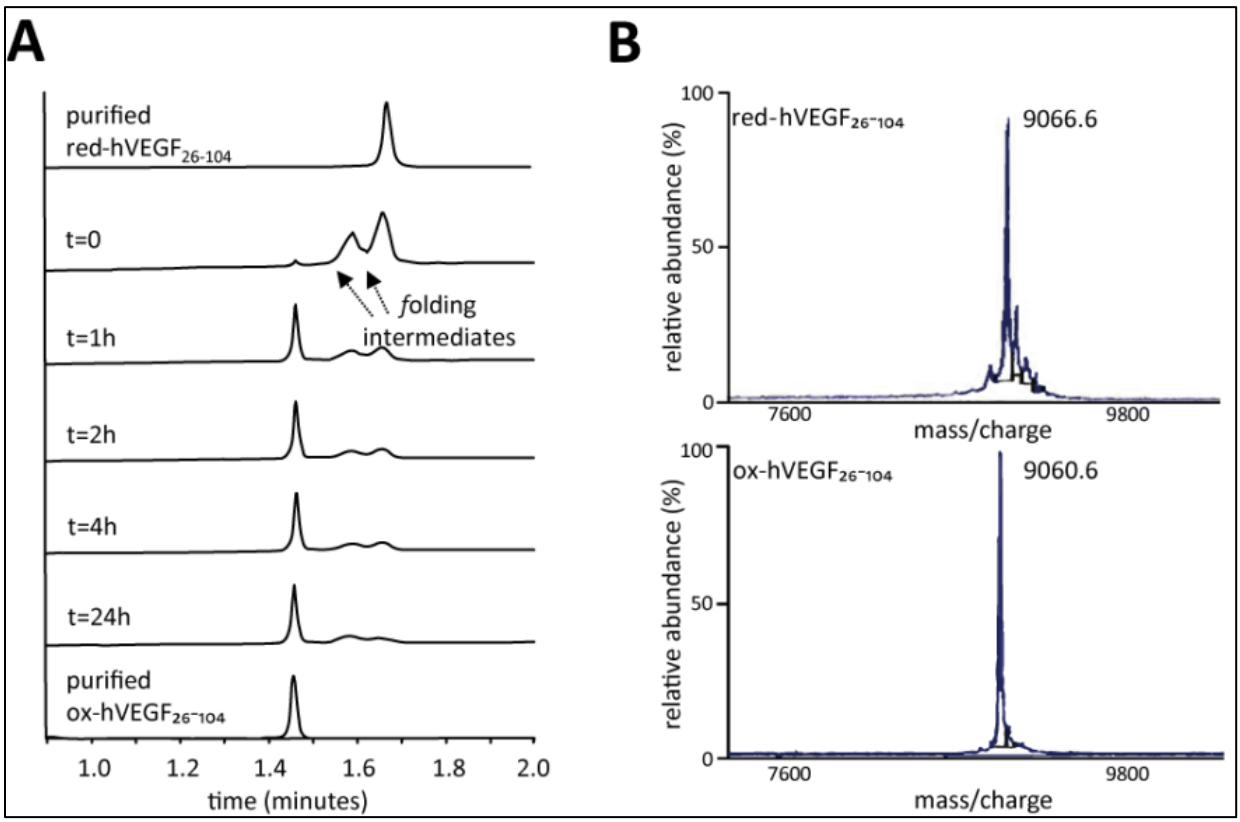

Fig. S1 Oxidative folding process of ox-hVEGF$_{26-104}$. UPLC-traces of the oxidative folding process of red-hVEGF$_{26-104}$ in folding buffer (pH 7.4) at 0, 1, 2, 4 and 24 hours (**A**). MALDI-ToF MS spectra of red-hVEGF$_{26-104}$ and ox-hVEGF$_{26-104}$ (**B**).

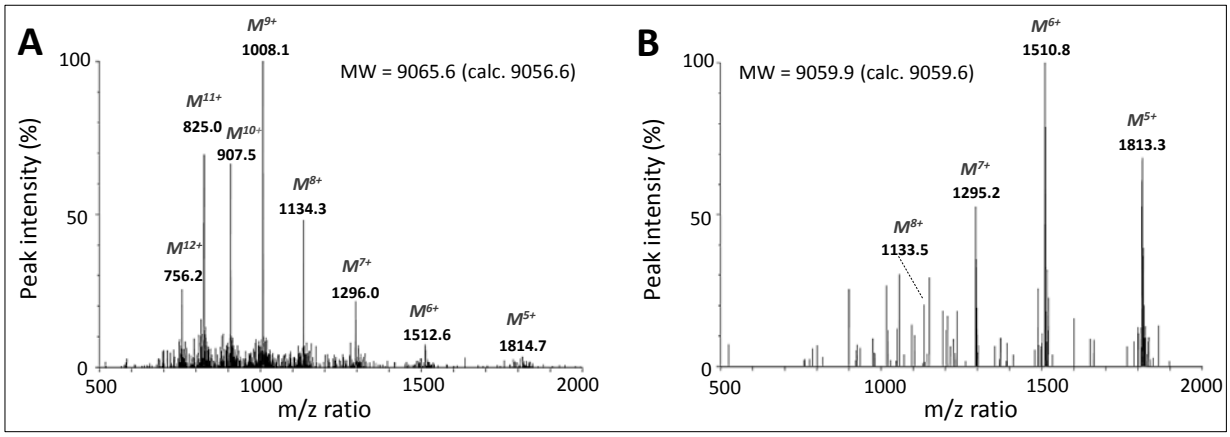

Fig. S2 ESI-MS spectra of red-hVEGF$_{26\text{-}104}$ (**A**) and ox-hVEGF$_{26\text{-}104}$ (**B**).

2. Activity studies of VEGF-mimics

2.1. Binding studies in ELISA

The binding of bevacizumab to peptides **1-33** was measured in ELISA (**Fig. S3**). Therefore, peptides were coated onto an ELISA-plate surface (10 µg/mL) and bevacizumab was subjected to bind to the peptide-coated surface. Of all human-VEGF derived peptides (**1-5**), the structured peptide **1** (3 native-SS; EC_{50} = 20-30 ng/mL) showed by far the strongest binding to bevacizumab. Binding of the 3 SS-deletion mutants **2-4** was much weaker and was also dependent on the position of the cys-knot SS-bond that had been deleted. Indeed, binding of peptide **3** (lacking the SS-bond that is closest to the bevacizumab-binding site) was undetectable at the highest concentration measured (pEC_{50}<2). However, binding of peptide **4** (i.e. SS-deletion variant-3, lacking the SS-bond that is furthest away from the bevacizumab-binding site) was the strongest of all 3 SS-deletion variants (pEC_{50}3.4), which is only ~16-fold lower than fully native peptide **1** itself (**Fig. S3A**). Interestingly, the rat- and mouse-variants of peptide **1** (i.e. peptides **6** and **7**) show no measurable binding to bevacizumab (see **Fig. S3B**), despite the fact that the sequences show ~90% sequence homology.

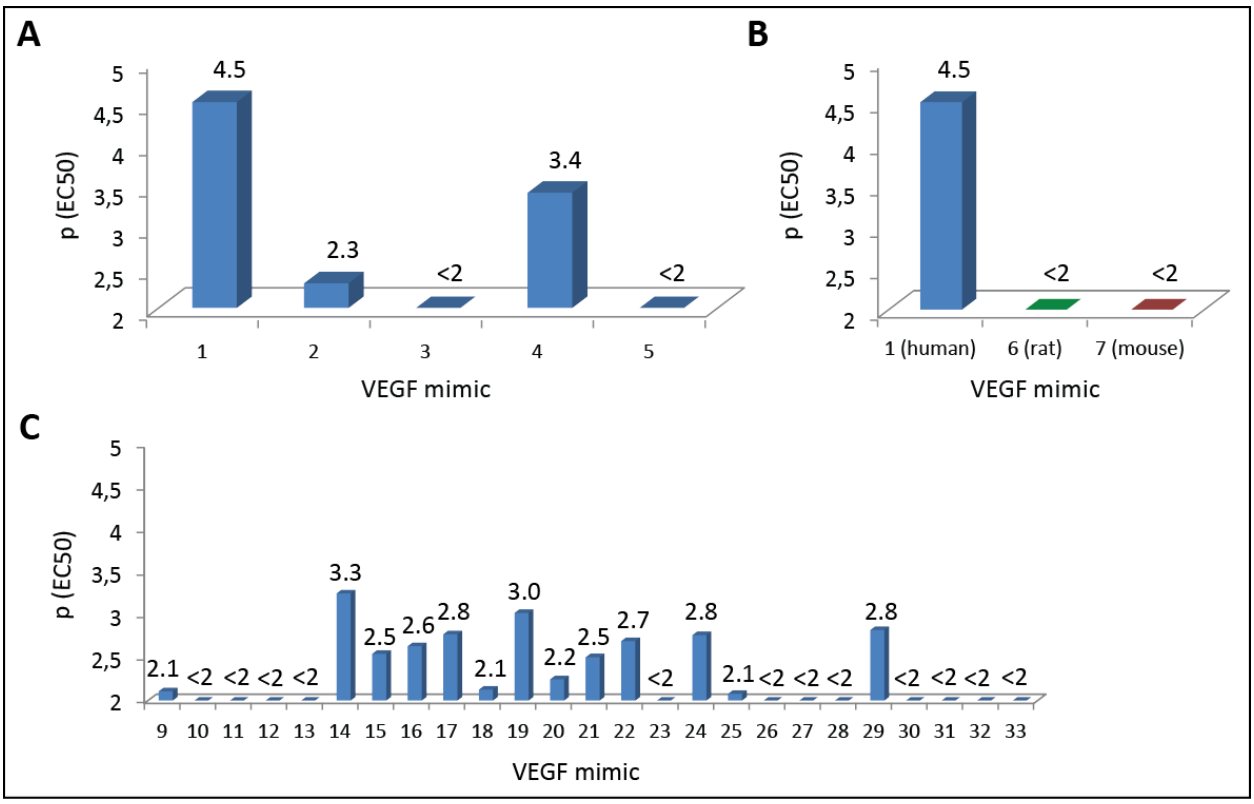

Figure S3 pEC50-values ($-^{10}\log[EC_{50}]$ values) for the binding of bevacizumab to (**A**) human-VEGF derived peptides **1-5**, (**B**) rat (**6**) and mouse (**7**) variant of peptide **1** (human) and (**C**) linear and cyclic peptides (**9-33**) in ELISA.

It was found that the linear β5-turn-β6 peptides **9-13**, nor the unstructured full-length $hVEGF_{26-104}$ **5** (IAM_6) showed measurable binding to bevacizumab up to a concentration of 10 µg/mL (**Fig. S3A, S3C**). Instead, the *meta*-xylene bridged peptides **14/19/24/29** displayed appreciable binding to bevacizumab (pEC_{50} between 2.8 and 3.3), which confirms the conformational nature of the bevaizumab binding site. Despite this, binding of the best peptides (**14/19**) is still ~16-fold weaker than for **1**, which exemplifies that insertion of the *meta*-xylene bridge is not able to enforce a similar 3D-structured epitope that is

comparable in binding strength to that obtained via formation of the cysteine-knot fold in combination with the structure-supporting β2-α2-β3-loop, as in peptide **1**.

Interestingly, bevacizumab binding to both peptide **14** and **19** strongly decreases upon further elongating the peptide sequence either at the C- or the N-terminal ends, with complete loss of binding for those peptides where the xylene-bridge was positioned at C_{80}-C_{92} (peptides **25-28**) or at C_{81}-C_{91} (peptides **30-33**). It is likely the introduction of an extra acidic residue (E_{72} or E_{103}), carrying a net negative charge at neutral pH, which makes bevacizumab-binding drop drastically (e.g. for peptides **15**, **18**, **20** and **23**). This is by no means due to a weakened 1:1 binding interaction between bevacizumab and the peptide, but rather due to a repulsive force between antibody and peptide that is characteristic for a high-density peptide-coated surface.

2.2 BIACORE affinity measurements

BIACORE affinity measurements were performed on a Biacore2000 instrument (GE Healthcare Biacore, Uppsala, Sweden). Running buffer was HBS-P20 (10 mM Hepes, 150 mM NaCl, 3.4 mM EDTA, 0.005% P20). Biotinylated $VEGF_{26\text{-}104}$ (biotinGGGC_{26}…C_{104}) was immobilized at levels 8 and 40 RU onto two channels of a CM5 chip coated with streptavidin. The reference surface contained only streptavidin. For affinity determinations, the antibody (bevacizumab and mAb 293 in concentrations ranges, respectively, 10-320 nM and 1-32 nM) was injected on reference and VEGF surfaces containing 5 to 40 RU of VEGF. Injection and post-injection phases lasted 1 and 5 min, respectively. After reference subtraction, sets of binding curves were evaluated by global fitting to either the bivalent analyte or Langmuir binding models, using the BiaEvaluation 4.1 software (GE-Healthcare Biacore).

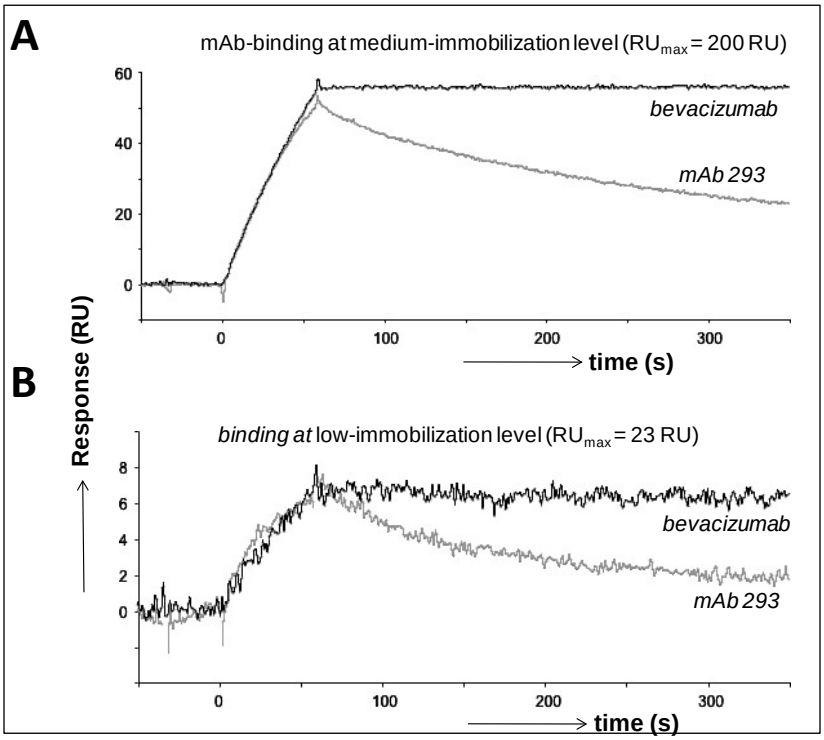

Figure S4. Kinetic curves for the binding of the humanized mAb bevacizumab (80 nM) and the murine mAb 293 (32 nM) to streptavidine-captured peptide **1** at (**A**) medium-immobilization level (R_{max} = 200 RU) and (**B**) low immobilization level; R_{max} = 23 RU),

showing a higher stability of the bevacizumab–VEGF compared to the mAb 293-VEGF complex.

Fig S5 shows the kinetic curves for the binding of (**A**) bevacizumab, and (**B**) mAb 293 to streptavidine-captured peptide **1** (mediumimmobilization level), showing again a higher stability of the bevacizumab●peptide **1** compared to the mAb 293● peptide **1** complex. Fitted curves using the Langmuir binding model are shown in black; the Chi2 was < 3% of R_{max}. The following rate parameters were calculated: Bevacizumab: k_{on} = 1.3(±0.4)x10^5 $M^{-1}s^{-1}$; k_{off}=0.9(±0.7) x 10^{-4} s^{-1} (mean of four experiments). mAb 293: k_{on} = 1.2(±0.3)x10^6 $M^{-1}s^{-}$, k_{off}=3.9(±1.1) x 10^{-3} s^{-1} (mean of two experiments). Calculation of k_{on} is based on total antibody concentration.

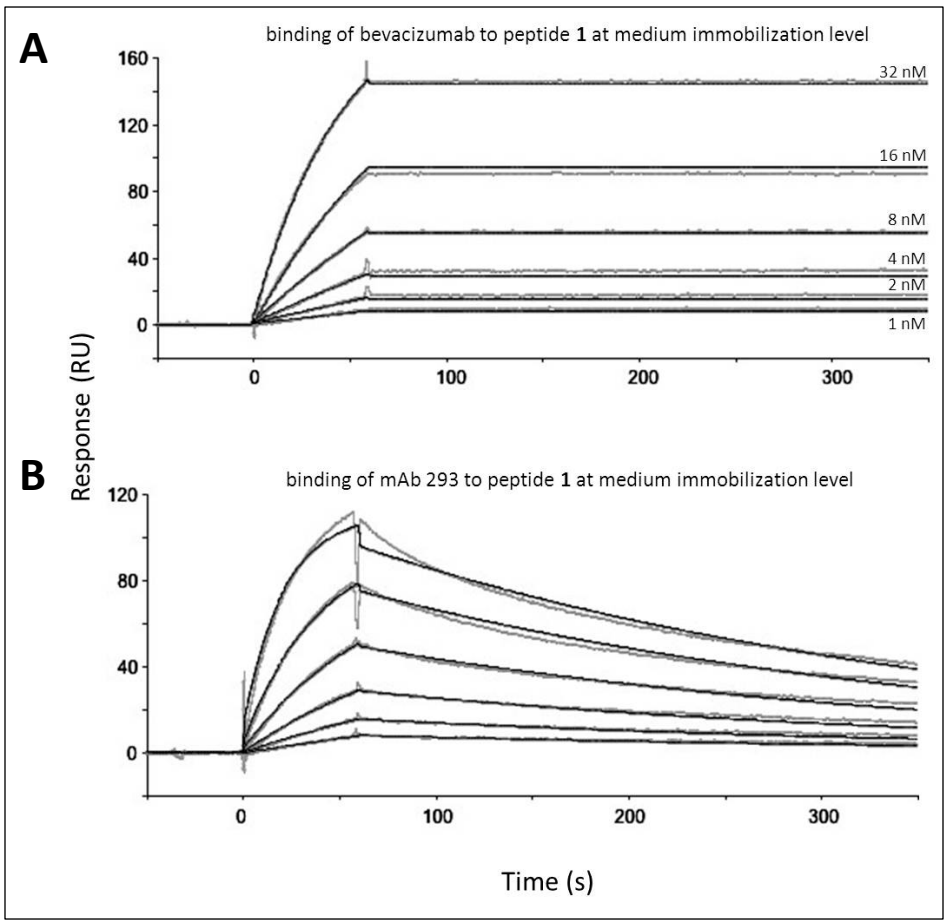

Figure S5 Sets of binding curves recorded with bevacizumab (**A**) and mAb293 (**B**) on a surface coated with peptide **1** (medium immobilization level: R_{max} = 200 RU).

2.3. Circular Dichroism (CD) spectroscopy studies

CD spectroscopy studies were carried out with peptides **1-5** in order to elucidate their structure in solution. The most relevant question was to clarify to what extent each individual SS-bond from the cys-knot fold contributes to overall binding. Furthermore, we wanted to assess how the overall stability of peptide **1** would change structure as result of an external stimulus, e.g. a switch in pH. Therefore, we studied peptides **1-5** at two different pH's, i.e. pH 4.0 and 7.5.

Peptides **1** and **4** are the only peptides that clearly showed a CD-spectrum that is different from a mere random coil structure (**Fig. S6**). The CD spectrum of peptide **1** displays a strongly positive CD around 200 nm and a weak negative CD around 215 nm, distinctly different from the characteristic minimum for random coil structures around 200 nm. Interestingly, the SS-del3 mutant peptide **4**, that lacks the lower cys-knot SS-bond (double Cys_{61}/Cys_{104}-A mutation), shows a CD spectrum very similar to that of **1** at pH 7.5 (**Fig. S6A**). However, at the lower pH of 4.0 the CD-spectrum of **4** has undergone a clear change and largely resembles the CD of a random-coil peptide **5**, while the CD-spectrum of **1** is virtually unchanged (**Fig. S6C**). This emphasizes the significantly lower stability of the partial cys-knot fold in SS-del-3 mutant peptide **4** (that has only two intact SS-bonds in the fold).

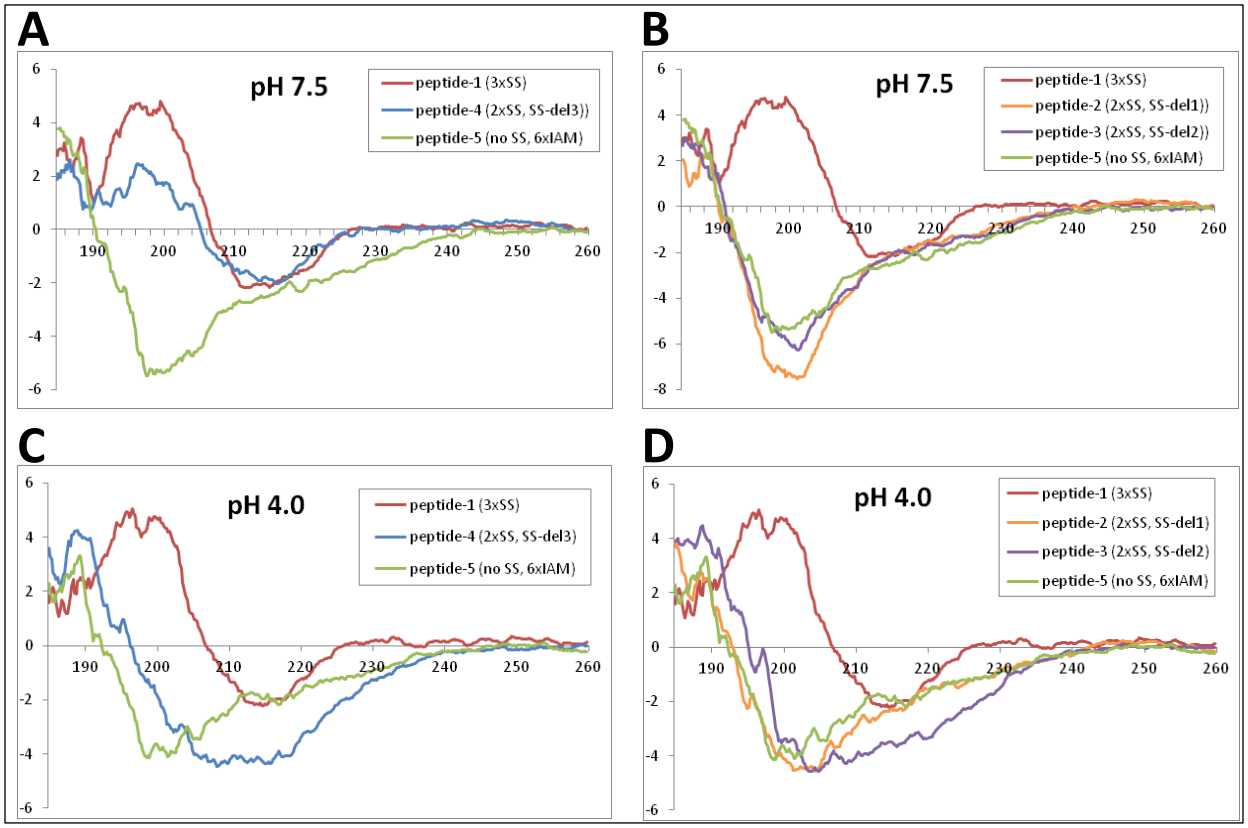

Figure S6 CD Spectroscopy studies for VEGF peptides **1-5** in aqueous solution at pH 7.5 (**A-B**) and pH 4.0 (**C-D**).

The two other SS-deletion mutants **2** (SS-del1, double Cys_{26}/Cys_{68}-A mutation) and **3** (SS-del2, double Cys_{61}/Cys_{102}-A mutation) mainly show random coil structures in solution at both pH 4.0 and 7.5 (**Fig. S6B** and **S6D**). These data perfectly agree with the observed low (**2**; pEC_{50} =2.25) or non-binding (**3**; pEC_{50} <2) of bevacizumab in ELISA (**Fig. S3A**), and highlight the importance of intact disulfide bonds in order to obtain a stable and correctly folded 3D-structure that adequately mimics the 3D-structure of endogenous $hVEGF_{165}$.

3. Peptide Immunization Studies

3.1 Overview of animal experiments

A number of different immunization studies were carried out using the VEGF-derived peptides **1-33** as immunogens. An overview of relevant studies is given below (**Table S4**).

Table S4. Overview of VEGF-peptide immunization experiments

Animal Nr.	Species (gender)	type animal	VEGF-peptide	Quantity (mgs)	Protein carrier	Adjuvant	Immunization schedule (wks)	Purpose
1-2	rat (m)	Wistar	1	3 x 0,25	n.a.	SFASE	0,2,4 (bl. 9)[#]	test immunogenicity
3-4	mouse (f)	Balb/C	1	2 x 0,25	n.a.	CFA/IFA	0,4 (bl. 7)	test immunogenicity
5-6	mouse (f)	Balb/C	1	3 x 0,25	n.a.	SFASE	0,2,4 (bl. 9)	test immunogenicity
7-8	rat (m)	Wistar	1	4 x 0,25	n.a.	SFASE	0,2,4,7 (bl. 9)	test immunogenicity
9-10	rat (m)	Wistar	2	4 x 0,25	n.a.	SFASE	0,2,4,7 (bl. 9)	test immunogenicity
11-12	rat (m)	Wistar	3	4 x 0,25	n.a.	SFASE	0,2,4,7 (bl. 9)	test immunogenicity
13-14	rat (m)	Wistar	4	4 x 0,25	n.a.	SFASE	0,2,4,7 (bl. 9)	test immunogenicity
15-16	rat (m)	Wistar	5	4 x 0,25	n.a.	SFASE	0,2,4,7 (bl. 9)	test immunogenicity
17-18	rat (m)	Wistar	6	4 x 0,25	n.a.	SFASE	0,2,4,7 (bl. 9)	test immunogenicity
19-28	rat (m)	Wistar	1	3 x 0,25	n.a.	CFA/IFA	0,4,7 (bl. 9)	Passive tumor-inhibition study-1
29-38	rat (m)	Wistar	1	4 x 0,25	n.a.	SFASE	0,2,4,7 (bl. 9)	Passive tumor-inhibition study-1
39-43	mouse (f)	Balb/C	1	4 x 0,25	n.a.	RFASE	0,2,4,7 (bl. 9)	test immunogenicity
44-48	mouse (f)	Balb/C	6	4 x 0,25	n.a.	RFASE	0,2,4,7 (bl. 9)	test immunogenicity
49-53	mouse (f)	C57BL6	1	4 x 0,25	n.a.	RFASE	0,2,4,7 (bl. 9)	test immunogenicity
54-58	mouse (f)	C57BL6	6	4 x 0,25	n.a.	RFASE	0,2,4,7 (bl. 9)	test immunogenicity
59-68	mouse (f)	Balb/C	1	4 x 0,25	n.a.	RFASE	0,2,4,6	Active tumor inhibition study-3
69-78	mouse (f)	Balb/C	7	4 x 0,25	n.a.	RFASE	0,2,4,6	Active tumor inhibition study-3
79-88	mouse (f)	Balb/C	8	4 x 0,25	n.a.	RFASE	0,2,4,6	Active tumor inhibition study-3
89-138	rat (m)	Wistar	9-33	2 x 1,0	n.a.	CFA/IFA	0,4 (bl. 7)	test immunogenicity
139-148	rat (m)	Wistar	15	2 x 1,0	n.a.	CFA/IFA	0,4 (bl. 7)	Passive tumor-inhibition study-2
149-158	rat (m)	Wistar	20	2 x 1,0	n.a.	CFA/IFA	0,4 (bl. 7)	Passive tumor inhibition study-2
159-168	rat (m)	Wistar	20*	2 x 1,0	KLH	CFA/IFA	0,4 (bl. 7)	Passive tumor-inhibition study-2

** a structural variant of peptide **20** was used, in which the normal meta-xylyl template was replaced by a meta-xylyl template that was functionalized at the remaining meta ring-position with a bromomethyl functionality that has been reacted with one molecule of 1,4-DTT. The resulting molecule that carries a free thiol-group (from the 1,4-DTT moiety) was conjugated to a KLH-carrier by means of sMBS-coupling chemistry.*

[#]bl means bleeding for serum collection

3.2 Choice of vaccine adjuvant and vaccine preparation

For the immunogenicity studies and the studies investigating the tumor inhibition potential (passive tumor inhibition study-1, passive tumor inhibition study-2, active tumor inhibition study-3), different adjuvants were used. Since CFA/IFA is not being used in clinical studies, we sought to find to a potent vaccine adjuvant with a good safety profile. SFASE adjuvant as well as the later developed RFASE adjuvant work as antigen depot, immune stimulators and skew the immune response towards humoral

immunity (4)(5). Initially, SFASE was developed and used in the immunogenicity studies as well as passive immunization studies 1 and 2, where it was compared to CFA/IFA. Toxicity issues in a later performed clinical study using SFASE resulted in the search for a new vaccine adjuvant with less toxicity but similar abilities to induce high antibody titers. The in-structure closely related adjuvant RFASE proved to have such properties and was therefore used in active immunization study-3. Raffinose Fatty Acid Ester (RFASE) adjuvant comprises the sulpholipopolysaccharide RFASE (with raffinose as backbone) in a submicron oil (squalane) in water emulsion. The sucrose fatty acid ester (SFASE) adjuvant comprises the sulpholipopolysaccharide SFASE (with sucrose as backbone) in a squalane in water emulsion (4, 5). Complete Freund's adjuvant (CFA) and Incomplete Freund's Adjuvant (IFA) were purchased at Sigma-Aldrich (Saint-Louis, MO). For the immunogenicity tests and active tumor-inhibition study-3, VEGF peptides were diluted in PBS to the appropriate concentration. Directly prior to immunization the VEGF peptides were mixed with the adjuvant. The final emulsion was homogenized by gently shaking.

3.3 Binding studies in ELISA/antibody titer determinations

3.3.1 Anti-VEGF antibody titer and VEGF concentration determination

For analysis of anti-VEGF antibodies, blood samples were left to coagulate overnight at 4°C and centrifuged twice at 7,000 RPM for 10 minutes. The supernatant was collected and stored at -80°C until use. Polystyrene Greiner 96-well plates (SIGMA-ALDRICH, St. Louis, MO) were coated with human or mouse VEGF carrier-free (CF) (1 µg/mL in PBS; PeproTech, London, UK) overnight at room temperature. After washing, the plates were blocked with horse serum (4% in PBS; SIGMA-ALDRICH, St. Louis, MO) for 2 hours. After washing, the plates were incubated for 2 hours with serum from either control or vaccinated mice, starting with 1:30 dilution in the first well and 3-fold dilution steps in subsequent wells. Then, the plates were incubated with Horse Radish Peroxidase (HRP)-conjugated secondary antibody (rabbit-anti-mouse IgG (1:1,000 dilution) or goat-anti-rat IgG (1:1,000 dilution; Southern Biotech, Birmingham, AL). HRP activity was detected by incubation with TMB (mouse sera) or ABTS (rat sera). The reaction was stopped by the addition of 2N H_2SO_4. The OD was measured with a TecanSpectrafluor plate reader at a wavelength of 450 nm and a reference wavelength of 540 nm for TMB and a wavelength of 405 nm and a reference wavelength of 490 nm for ABTS. Anti-VEGF antibody titers were calculated by determining the serum dilution at which the OD was equal to 4*OD of the negative control (4% horse serum in PBS). The titer defines the negative ^{10}log-value of the dilution factor. For active-immunization study-3, serum $mVEGF_{164}$ concentrations were measured in duplicate by sandwich ELISA (R&D systems, Minneapolis, USA) according to the manufacturers' directions.

*3.3.2 Hyper immune sera elicited against 'VEGF-trunc' peptides **1-6***

Using different administration routes, immunization with peptide **1** elicited high titers of antibodies against peptide 1 and full length hVEGF (**Table S5**). Immunization with the rat homolog of peptide **1** (ox-rVEGF26-104; peptide **6**) induced similar antibody titers, which were also cross-reactive with full length rVEGF (**Table S6**). This indicates that immunization with a peptide from the same species is still able to induce a potent antibody response. Immunization with peptides **2-5** (SS deletion variants and unfolded variant of peptide **1**) similarly resulted in high antibody titers (**Table S7**). However, these antibodies appeared to be non-neutralizing as no inhibition of VEGF dependent Ba/F3-VEGFR2 cell proliferation was found.

Table S5. Antibody titers (^{10}log[dilution factor]) for sera 1-2 (Wistar rats) and sera 3-6 (Balb/C mice) elicited against structured peptide **1** (human) and full length hVEGF

Animal nr.	VEGF peptide	Adjuvant	Mode of immunization	Ab titer				
				Week 0	**Week 6**	**Week 0**	**Week 4**	***Week 6***
				Peptide 1		hVEGF		
1	1	SFASE	im/sc 50/50	<2	-	<2	3.3	5.2
2	1	SFASE	im/sc 50/50	<2	-	<2	4.4	>5.4
3	1	CFA/IFA	ip/sc 50/50	<2	4.7	<2	-	5.3
4	1	CFA/IFA	ip/sc 50/50	<2	4.6	<2	-	5.2
5	1	SFASE	ip	<2	5.1	<2	-	5.4
6	1	SFASE	Ip	<2	5.1	<2	-	5.3
Beva (0.5 µg/mL)		n.a.	n.a.	3.3		4.2		

Table S6. Antibody titers (^{10}log[dilution factor) in Wistar rats immunized with peptide **1** (serum 8) and peptide **6** (17-18) elicited against peptide **1**, peptide **6**, full length hVEGF and rVEGF.

Animal nr.	VEGF peptide	Adjuvant	Mode of immunization	Ab titer 9 weeks after primer immunization			
				Peptide 1	Peptide 6	hVEGF	rVEGF
8	1	SFASE	ip	5.3	5.3	4.9	4.0
17	6	SFASE	ip	-	-	5.1	4.6
18	6	SFASE	ip	>5.4	5.1	5.1	-
Beva (1.0 µg/mL)		n.a.	n.a.	3.8	<1	4.1	<1

Table S7. Antibody titers (^{10}log[dilution factor]) for antisera elicited against SS-deletion variants **2-5**
* Serum of week 9 was purified and used in 1:50 dilution

Animal nr.	VEGF peptide	Adjuvant	Mode of immunization	Ab titer 9 weeks after primer immunization						Ba/F3-VEGFR2 cell proliferation (% of positive control)*
				Peptide 1	Peptide 2	Peptide 3	Peptide 4	Peptide 5	hVEGF	
8	1	SFASE	ip	>5.4	3.6	3.4	5.3	3.9	5.1	48
9	2	SFASE	ip	5.0	5.3	5.3	5.3	5.4	4.4	128
10	2	SFASE	ip	5.3	>5.4	>5.4	5.4	>5.4	4.5	106
11	3	SFASE	ip	5.3	5.2	5.3	5.3	5.4	4.7	110
12	3	SFASE	ip	5.4	>5.4	>5.4	>5.4	>5.4	4.7	99
13	4	SFASE	ip	5.4	5.4	5.4	>5.4	>5.4	4.8	86
14	4	SFASE	ip	5.3	>5.4	5.4	5.4	>5.4	4.7	96
15	5	SFASE	ip	5.3	5.3	5.4	5.3	5.4	4.6	109
16	5	SFASE	ip	5.2	5.4	5.4	5.4	>5.4	4.7	88
Beva (1.0 µg/mL)		n.a.	n.a.	3.8	<1	<1	2.2	<1	4.1	38

*3.3.3. Anti-VEGF antibody titers induced by immunization with peptides **9-33***

Immunization with linear and cyclized peptides (**9-33**) in general elicited high titers of antibodies against hVEGF. However, the peptides cyclized between residues 81-91 seemed to be less effective, as this resulted in lower antibody titers (**Fig. S7**).

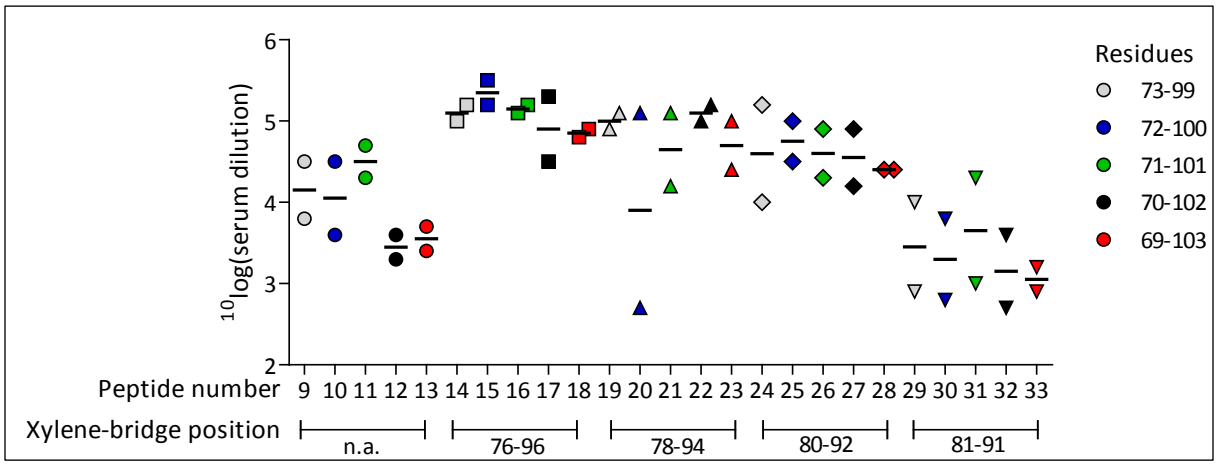

Figure S7 Antibody titers (^{10}log(dilution factor)) for peptide antisera raised against the linear and cyclized peptides **9-33**. The titer gives the value at which antibody titers are calculated at an OD_{405nm} that is equal to 4x the background level (OD_{405nm} ~ 0.4 A.U.).

Table S8 Antibody titers (^{10}log[dilution factor]) for 30 antisera raised against the xylene-bridged peptides **15** and **20**. The most potent antisera were used for passive tumor-inhibition study-2 (see **section 3.5.1**).

Animal nr.	**Peptide number**	**Ab-titer (week 7) ($^{-10}$ log dilution) (mean±SD)**	**Ba/F3-VEGFR2 cell proliferation (% of positive control)**	
			Unpurified (mean±SD)	Purified (mean±SD)
139-148	15	4.1 (±0.4)	96.1 (±9.6)	77.8 (±12.7)
149-158	20	4.0 (±0.6)	94.2 (±9.7)	74.1 (±10.0)
159-168	20*	3.2 (±0.4)	78.6 (±14.7)	62.4 (±8.7)

3.4 Ba/F3-cell inhibition data of anti-peptide 1 antisera

The neutralizing abilities of two sera derived of rats immunized with peptide 1 were studied in detail using the Ba/F3-VEGFR2 cell proliferation assay. It was shown that non-purified sera could be diluted 400 times and still inhibited VEGF driven Ba/F3-VEGFR2 cell proliferation over 50% compared to $hVEGF_{1-165}$ 0.6 ng/mL (**Fig. S8**).

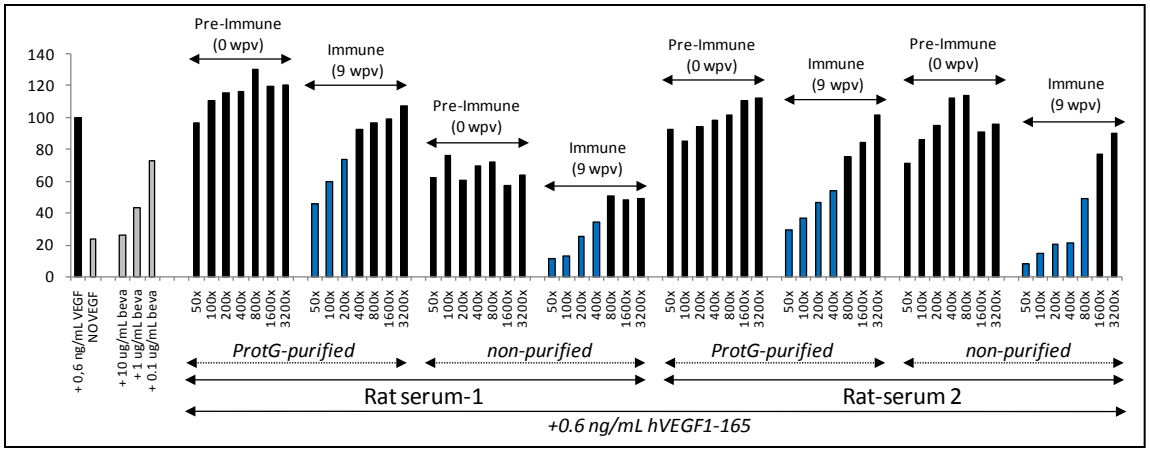

Figure S8 Inhibition data for rat serum-1 and 2 illustrating the strong in-vitro neutralizing ability of antisera raised against peptide **1**.

3.5 Tumor-growth inhibition studies

3.5.1 General Procedure for the passive immunization studies in LS174 T colon cancer bearing Swiss nu/nu mice (study 1+2)

In this study, male Wistar rats (nr. 19-38 for study 1 and nr. 139-168 for study 2; all purchased from Charles River Laboratories (Sulzfeld, Germany)) were immunized with the studied immunogen (for detailed information, see **Table S1** and **S4**). Two weeks after the last immunization the animals were bled, the blood fraction was centrifuged to remove all cellular components, and the IgG-fraction of the sera was isolated using ProtG-based affinity chromatography. The IgG-fraction was finally obtained by eluting the column with 5x less buffer (v/v) than the original blood volume. The most potent antisera (selected by comparison of the ELISA-competition data and VEGF neutralization data in the Ba/F3-VEGFR2 cell proliferation assay) were pooled and used for passive immunization of the tumor-bearing mice (Charles River, Wilmington, MA).

Thereafter, Swiss nu/nu mice (Charles River Laboratories, were challenged with $1.5*10^6$ LS174T human colon cancer cells and subsequently treated 3 times 500 µL of PBS (group-1), 5x concentrated antiserum (group-2) or bevacizumab (25 mg/mL, group-3) with one-week intervals. The tumors were allowed to grow for 26 days (data of passive study-1: **Fig. 4**; data of passive study-2: **Fig. S10**). Tumor sizes were measured every two days with a digital sliding caliper. Tumor volumes were calculated using the formula: volume = 0,5*length*width^2. After euthanization, the tumors were dissected free and stored at -80°C until further processing.

3.5.2 Procedure for the active immunization study in B16F10 melanoma bearing immunocompetent mice (study-3)

For the active immunization study C57BL/6 mice (Charles River Laboratories, Sulzfeld, Germany) were prophylactically immunized with 175 µL peptide-**8**/RFASE (group-3), peptide-**7**/RFASE (group-4), or peptide-**1**/RFASE (group-5). Control mice received either RFASE (group-2) or PBS (group-1) alone. The mice were immunized 4 times 2 weeks apart through intramuscular injections in the left and right hind leg. The given doses of peptide immunogen and adjuvant were 250 and 500 µg, respectively. Ten days after the last immunization the mice were challenged with $5*10^4$ B16F10 murine melanoma cells. The tumors were allowed to grow for 21 days (**Fig. 5A**). Hereafter, mice were euthanized and tumors were dissected free and stored at -80°C until further processing. Blood samples were taken the day before

tumor cell inoculation (t = -1 day) and on the day of euthanization (t = 21 days). The tumor volumes were calculated using the formula: volume = 0,5*length*width^2.

3.5.3 Safety data immunization studies 1-3 and efficacy results immunization study-2

One mouse in group-1 died before tumor inoculation and four mice in group-1 were sacrificed before the scheduled end of the study because the estimated tumor volume approached or exceeded 4000 mm^3. In study-2 there were no unscheduled deaths.

In neither of the passive immunization studies (studies 1 and 2) or the active immunization study (study-3), there was no significant weight loss after vaccination and tumor inoculation compared to the control groups (**Fig. S9**, **Fig. S10C**, **Fig. S11**), indicating that vaccination is devoid of gross toxicities.

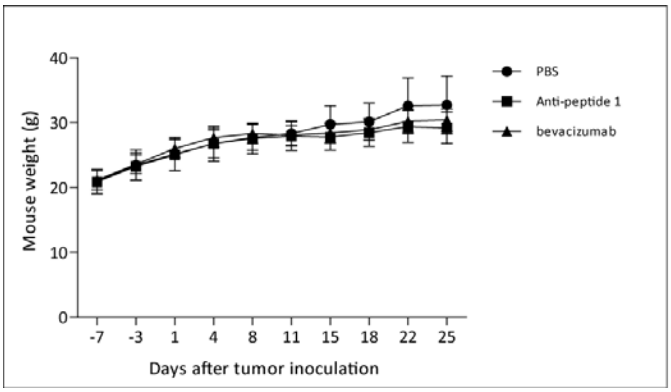

Fig. S9 Mouse weights in tumor-growth inhibition study 1, showing no toxic effects of treatments.

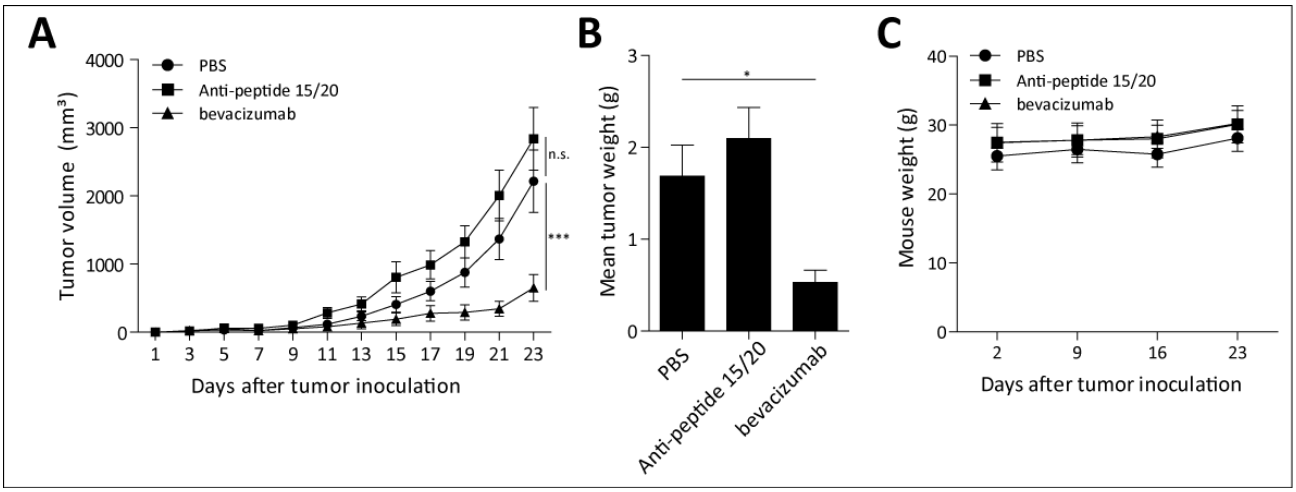

Fig. S10 Growth curves and weights of LS174T tumors in Swiss nu/nu mice (study 2), showing the inhibitory effect of bevacizumab treatment and no inhibitory effects of anti-peptides **15** and **20** antiserum in comparison to PBS treated mice (**A-B**). Data are expressed as mean ± SEM (*n* = 10 per group). Mice weights after tumor inoculation and treatments with PBS, anti-peptide 10/11 or bevacizumab, showing no toxic effects (**C**). Data are expressed as mean ± SD (*n* = 10 per group).

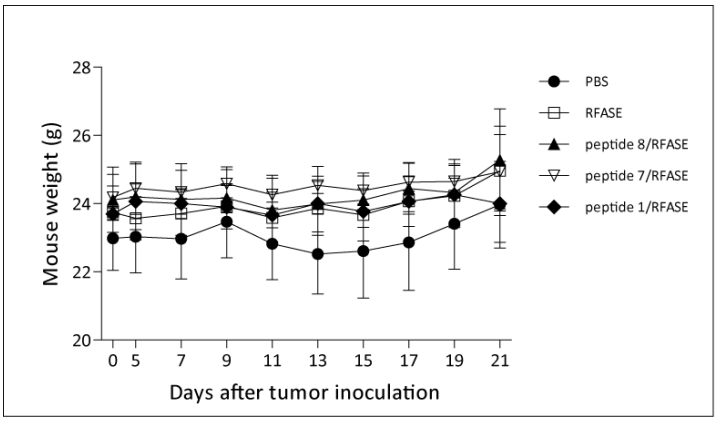

Fig. S11 Mouse weights in tumor-growth inhibition study 3, showing no toxic effects of treatments.

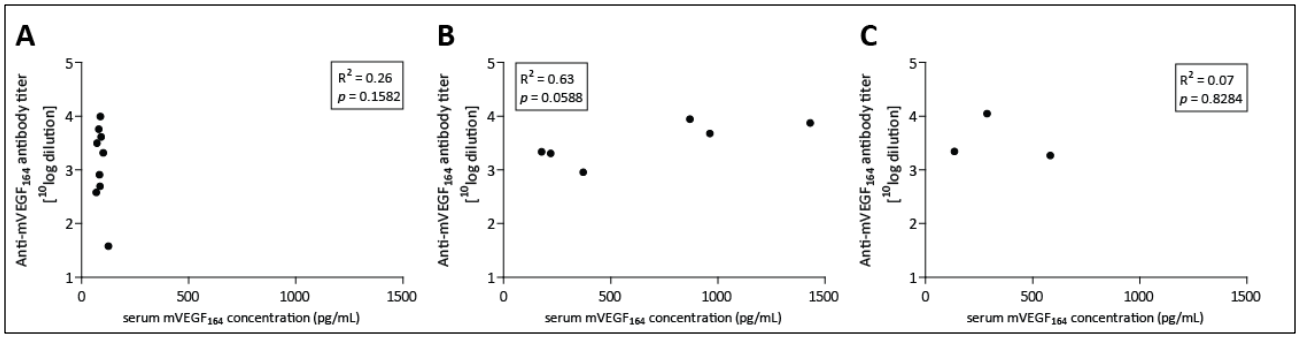

Fig. S12 Correlation plots between serum $mVEGF_{164}$ concentrations (X axis) and anti-$mVEGF_{164}$ antibody titers (Y axis) in tumor-growth inhibition study 3. Results are shown separately for mice immunized with peptide **8**/RFASE group-3, **A**), peptide **7**/RFASE (group-4, **B**) and peptide **1**/RFASE (group-5, **C**) and show a trend towards a significant correlation only in the group immunized with peptide **7**/RFASE.

References

1. Muller YA *et al* (1998) VEGF and the Fab fragment of a humanized neutralizing antibody: crystal structure of the complex at 2.4 A resolution and mutational analysis of the interface. *Structure* 6 (9): 1153-1167

2. Timmerman P, Beld J, Puijk WC, Meloen RH (2005) Rapid and quantitative cyclization of multiple peptide loops onto synthetic scaffolds for structural mimicry of protein surfaces. *Chembiochem* 6 (5): 821-824

3. Timmerman P, Puijk WC, Meloen RH (2007) Functional reconstruction and synthetic mimicry of a conformational epitope using CLIPS technology. *J Mol Recognit* 20 (5): 283-299

4. Blom AG, Hilgers LA (2004) Sucrose fatty acid sulphate esters as novel vaccine adjuvants: effect of the chemical composition. *Vaccine* 23 (6): 743-754

5. Hilgers LA, Blom AG (2006) Sucrose fatty acid sulphate esters as novel vaccine adjuvant. *Vaccine* 24 Suppl 2 S2